

# A High-Speed Master-Slave ADALINE for Accurate Power System Harmonic and Inter-Harmonic Estimation

PRIYABRAT GARANAYAK<sup>1</sup>, R. T. NAAYAGI<sup>2</sup>, (Senior Member, IEEE),  
AND GAYADHAR PANDA<sup>3</sup>, (Senior Member, IEEE)

<sup>1</sup>Indian Institute of Information Technology Una, Una 174303, India

<sup>2</sup>The Newcastle University in Singapore (NUIS), Singapore 567739

<sup>3</sup>National Institute of Technology at Meghalaya, Shillong 793003, India

Corresponding author: Priyabrat Garanayak (garanayak.priyabrat@gmail.com)

**ABSTRACT** This paper presents a unique two-fold adaptive linear neural network (ADALINE) for fast and accurate measurement of fundamental, harmonics, sub-harmonics, inter-harmonics and decaying DC components of a distorted current signal with additive noise. The preceding parallel approach is termed as Master-Slave ADALINE (MS ADALINE). The Slave-ADALINE adopts least mean square (LMS) algorithm with a fixed and large step-size for weight vector adjustment. During the training interval or transients, this filter performs a significant role. On the other hand, the Master-ADALINE uses a variable step-size LMS algorithm for achieving a small steady-state error. At the end of each iteration, the local averages of the squared errors of both the ADALINE's are calculated and weights of the Master-ADALINE are updated accordingly. The amplitudes and phases of desired frequency components can be worked out from Master-ADALINE's weights. The proposed architecture improves the convergence speed by establishing an independent control action between the steady-state error and the speed of convergence. The simulation results of this method under various operating situations are analyzed and compared with single fold ADALINE structure that obeys dynamic step-size LMS (DSSLMS) adaptation rule. Eventually, a scaled laboratory prototype has been developed for the validation of the proposed technique in real-time utilization. This innovative research finding makes the power system smart and precise.

**INDEX TERMS** Adaptive linear neural network (ADALINE), dynamic step-size least mean square (DSSLMS), harmonic estimation, power quality assessment, master-slave (MS).

## I. INTRODUCTION

The wide application of power converters using semiconductor devices controls the performance of many electrical and electronic equipment. Due to the switching mode operation, these nonlinear devices inject harmonics into the AC system. As a consequence, accurate measurement of the individual component is essential for power quality control and protection. Finding an efficient method for fast and accurate estimation of the parameters (i.e. amplitude, phase, and frequency) of the fundamental, harmonics, inter-harmonics, sub-harmonics and decaying DC components has become a large scale research area for power engineers and researchers.

The associate editor coordinating the review of this manuscript and approving it for publication was Mehdi Savaghebi<sup>1</sup>.

In the past, several approaches have been reported for parameter estimation, among them, Fast Fourier Transformation (FFT) is most commonly used due to its low computational complexity structure. However, the FFT based technique suffers from spectral leakage and poor convergence rate while determining sub- and inter-harmonic parameters [1]. Furthermore, this method is delayed by more than two fundamental periods because it takes one period for acquiring the data and another period for analysis of data [2]. Therefore, its performance gets deteriorated in real-time implementation.

A widely used method for parameter estimation is the least-squares (LS) technique, where the aim is to minimize the squared error between the measured and modelled signal [3]–[7]. The performance of the algorithm is affected by the width of the observation window, choice of the sampling

frequency, selection of reference time, and Taylor Series truncation. Pradhan *et al.* [8] and Subudhi *et al.* [9] suggested the LMS algorithm for power system frequency estimation. However, this method is not so effective for amplitude and phase estimation. On the other hand, the recursive least squares (RLS) technique is a well established numerical method which can deal effectively with decaying DC offsets, power system frequency transients and subsynchronous oscillations [10], [11]. However, the computational complexity of the RLS technique hinders its real-time implementation.

Another commonly used estimation technique is the Kalman filter (KF), as a recursive stochastic technique that gives an optimal estimation of state variables of a given dynamic system from noisy measurements [12]–[14]. The main drawback of this algorithm is the bulk calculations that limit its online application due to the requirement of large memory and high-speed microprocessor. This algorithm also fails to track abrupt or dynamic changes of the signal.

In the last couple of decades, many power system harmonic estimation techniques employing the learning principles have become quite popular. These techniques are applied to overcome the shortcomings such as inaccuracy on account of incorrect modelling, noise present in the signal and non-linearity. Jain and Singh [15] proposed an artificial neural network (ANN) to estimate the harmonic components accurately by taking 1/2 cycle sampled values of a distorted waveform in noisy environments. Abdeslam *et al.* [16] and Rodriguez *et al.* [17] have suggested a new approach using an adaptive linear neural network (ADALINE) for online harmonic estimation. In recent years, ADALINE structure is widely used as harmonic estimator due to its simple structure and nonstationary signal parameter tracking capability. It resolves the distorted current/voltage signal to its Fourier series. Goh *et al.* [18] developed a unified approach for mean square convergence analysis for ADALINE structure, including mean square stability, mean square evolution (transient behaviour) and the mean square steady-state performance. Recently, Chang *et al.* [19] proposed two-stage ADALINE that is robust and capable of detecting harmonics and inter-harmonics. Sarkar *et al.* [20] proposed a modified ADALINE structure, namely self-synchronized ADALINE (S-ADALINE) provides faster response and better noise immunity than the conventional ADALINE structure. Garanayak and Panda [21] proposed a hybrid ADALINE and filtered-x LMS technique to overcome the error in estimation under highly impulsive noise. Some well documented harmonic estimation approaches using ADALINE structures along with weight updating rule provide accuracy and reduce response time [22]–[24]. This multi-input and single output architecture provides low complexity design structure, minimum tracking error and faster convergence rate.

In general, the weights/coefficients of the ADALINE are updated by the LMS adaptation rule due to its simple structure and robustness. The step-size parameter is critical to the performance of the LMS algorithm and evaluates how fast the algorithm converges along the error

performance surface. To accelerate the speed of convergence and minimize the excess mean squared error (MSE), several time-varying step-size techniques have been reported in the literature [25]–[32]. The basic principle is that at the starting stages of convergence or transients, the step-size parameter should be large, in order to achieve a faster convergence rate and minimum error. After a number of iterations, the filter coefficients are closer to the optimum solution; a minimum step-size value should be used for attaining a small steady-state error [28], [29]. Adaptation of step-size highly depends on a few parameters like instantaneous square error, error autocorrelation and change in the sign of gradient between the input signal and output error. In addition, the steady-state misadjustment depends on all constant parameters, thus the dependence between the speed of convergence and the steady-state error exist [30]–[33]. For these reasons, ADALINE followed by variable step-size LMS learning rule converges prematurely during the estimation of the signal having time-varying parameters, decaying DC function, high-level measurement noise and inter-harmonics. As a result, the accuracy of the estimation gets reduced, which is the main disadvantage of conventional methods.

This paper contributes to a new Master-Slave ADALINE (MS ADALINE) based two-fold architecture for real-time detection of grid voltage/current fundamental and harmonic components. This method theoretically cancels out the dependency between the speed of convergence and steady-state errors, and at the same time enhances the convergence speed. In MS ADALINE technique, two ADALINE modules, i.e. Master-ADALINE and Slave-ADALINE are connected in parallel. The reference signals are applied to both ADALINE, i.e. common parallel input and the error outputs are collected independently, i.e. parallel output. The Slave-ADALINE's coefficients are updated by the fixed step-size LMS algorithm. Just to speed up the convergence, large step-size value is a prominent choice. During the training interval or sudden parameter changes, this filter coefficients close near to the optimum solution. On the other hand, the Master-ADALINE chooses a time variable step-size LMS algorithm for coefficient adjustment. When this algorithm goes closer to the steady-state, the value of error magnitude reduces, which decreases the step-size. In the meantime, the obtained filter coefficients are optimum. At the end of each iteration, the local averages of the squared errors of both the ADALINE's are computed and applied to the decision control circuit. Then, the decision controller circuit compares the two magnitudes and adjusts the Master-ADALINE weights accordingly. In this way, the system can overcome the effect of estimation error with a large magnitude by using MS ADALINE. The Master-ADALINE is the filter of interest, and from its coefficients, the amplitudes and phases are estimated. The proposed architecture provides the fastest convergence speed and smallest steady-state error than the single-fold ADALINE structure with a low increase in computational complexity. It has the advantage to estimate the vibration harmonic magnitude and phase with high tracking accuracy. It can be easily

expected that the performance of the recommended architecture would be better than that of simple ADALINE structure. This approach is not only used for power quality assessment in the electrical system but also it can be implemented in other research fields like equalization, active noise control (ANC), acoustic echo cancellation and biomedical engineering.

In the simulation, we assumed a test signal that contains fundamental, harmonics, inter-harmonics, sub-harmonics, decaying DC components and random noise. By using the adaptive technique, we have estimated the parameters of these components. Then, these estimated values are compared with the actual values to evaluate the percentage errors. But for experimental analysis, we have collected the discrete values of nonlinear current from the laboratory prototype. This distorted current is considered as a test signal for estimation. For validation of the proposed algorithm in a real-time environment, the parameters of the individual component present in a test signal are estimated and compared.

## II. ARCHITECTURE OF SINGLE FOLD ADALINE STRUCTURE

A periodic and distorted current  $i(t)$  can be described by the sum of the fundamental frequency and integral multiples of the fundamental frequency (i.e. harmonics) with unknown amplitudes and phases. It is assumed that frequency is known and constant during the estimation process. The discrete-time version of  $i(t)$  can be expressed as follows.

$$\begin{aligned}
 i(n) &= \sum_{i=1}^L I_i \sin(\omega_i n + \Phi_i) \\
 &= \sum_{i=1}^L [I_i \cos \Phi_i \quad I_i \sin \Phi_i] \begin{bmatrix} \sin \omega_i n \\ \cos \omega_i n \end{bmatrix} \\
 &= \sum_{i=1}^L [a_i \quad b_i] \begin{bmatrix} x_{ai}(n) \\ x_{bi}(n) \end{bmatrix} \tag{1}
 \end{aligned}$$

where  $\omega_i$ ,  $I_i$  and  $\Phi_i$  represent the angular frequency, amplitude and phase angle of  $i^{th}$  components respectively.  $\{a_i = I_i \cos \Phi_i, b_i = I_i \sin \Phi_i\}_{i=1}^L$  denote discrete Fourier coefficients of the fundamental and harmonic components, respectively. References  $\{x_{ai}(n) = \sin \omega_i n, x_{bi}(n) = \cos \omega_i n\}_{i=1}^L$ , are generated from the phase-locked loop (PLL) circuit.

The functional block diagram of single fold ADALINE for harmonic parameter estimation is depicted in Fig. 1. It is composed of  $2L$  number of neurons, whose weight vector  $w = \{\hat{a}_i(n), \hat{b}_i(n)\}_{i=1}^L$  is adjusted by dynamic step-size LMS (DSSLMS) algorithm [21], [27], [29]. The reference inputs are  $\{x_{ai}(n), x_{bi}(n)\}_{i=1}^L$ . The control signal  $y(n)$ , which is the algebraic sum of all the filter outputs, can be derived as

$$y(n) = \sum_{i=1}^L (y_i(n)) = \sum_{i=1}^L [\hat{a}_i(n) \quad \hat{b}_i(n)] \begin{bmatrix} x_{ai}(n) \\ x_{bi}(n) \end{bmatrix} \tag{2}$$

The preceding equation can be written in matrix form as

$$y(n) = w^T(n)x(n) \tag{3}$$

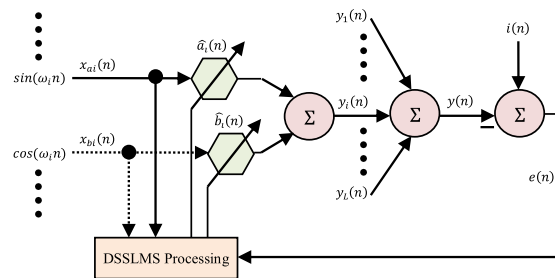


FIGURE 1. Functional block diagram of single fold ADALINE structure.

Then, the instantaneous error  $e(n)$  is the difference between the sensed signal  $i(n)$  and the control signal  $y(n)$ . Accordingly, we can write

$$e(n) = i(n) - w^T(n)x(n) \tag{4}$$

After a number of iterations, the estimated amplitudes  $\{I_i\}_{i=1}^L$  and phases  $\{\Phi_i\}_{i=1}^L$  can be computed as follows.

$$I_i = \sqrt{\hat{a}_i(n)^2 + \hat{b}_i(n)^2} \tag{5}$$

$$\Phi_i = \tan^{-1}(\hat{b}_i(n)/\hat{a}_i(n)) \tag{6}$$

### A. DSSLMS WEIGHT UPDATING RULE

By employing DSSLMS algorithm, the estimated coefficients  $\{\hat{a}_i(n), \hat{b}_i(n)\}_{i=1}^L$  at any sampling instant  $n$  are updated by using the following expressions.

$$\begin{aligned}
 \hat{a}_i(n+1) &= \hat{a}_i(n) + \mu_{ai}(n) e(n) x_{ai}(n) \\
 \hat{b}_i(n+1) &= \hat{b}_i(n) + \mu_{bi}(n) e(n) x_{bi}(n) \tag{7}
 \end{aligned}$$

where  $\mu_{ai}(n) = \mu_{bi}(n) = \mu_i(n)$  represents the time-varying step-size parameters that can be adapted as

$$\mu'_i(n+1) = C_1 \mu_i(n) + C_2 p^2(n) \tag{8}$$

$$\mu_i(n+1) = \begin{cases} \mu_{max}, & \text{if } \mu'_i(n+1) > \mu_{max} \\ \mu_{min}, & \text{if } \mu'_i(n+1) < \mu_{min} \\ \mu'_i(n+1), & \text{else} \end{cases} \tag{9}$$

where  $(0 < C_1 < 1)$  and  $(C_2 > 0)$  are constant values to control the convergence rate, and  $\mu_i(n+1)$  is restricted in some pre-decided  $[\mu_{min}, \mu_{max}]$  to provide stability and learning behaviour of DSSLMS algorithm. The error autocorrelation  $p(n)$  can be expressed as

$$p(n) = C_3 p(n-1) + (1 - C_3) e(n)e(n-1) \tag{10}$$

where  $(0 < C_3 < 1)$  is an exponential weighting factor that controls the quality of the estimation of  $p(n)$ . From Eq. (8) and Eq. (10), it is seen that the autocorrelation between the error output at adjacent time instants  $e(n)$  and  $e(n-1)$  regulate the step-size parameter. Therefore, the influence of the measurement noise is reduced and the algorithm performs better at the steady-state condition.

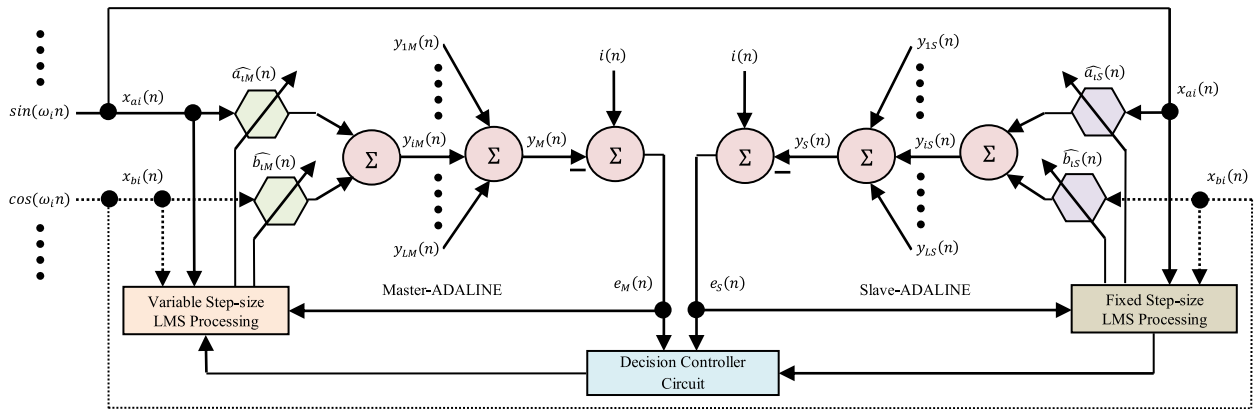


FIGURE 2. Functional block diagram of proposed two fold MS ADALINE structure.

**B. MISADJUSTMENT LEVEL**

The steady-state performance of the adaptive algorithm is commonly measured using a relative parameter, called misadjustment. It is defined as the ratio of the steady-state excess MSE function  $J_{ex}(n)$  to the optimal MSE  $J_o$ . Referring [31], the steady-state misadjustment level  $\mathcal{M}$  is calculated as

$$\mathcal{M} = \frac{C_1 C_2 J_o^2 (1 - C_3)}{(1 - C_1^2)(1 + C_3)} tr[R] \tag{11}$$

where  $tr[\cdot]$  represents the trace of the matrix  $(\cdot)$  and  $R$  is the input autocorrelation matrix given by  $R = EX(n)X^T(n)$ . The preceding equation states that  $\mathcal{M}$  depends on all constant parameters ( $C_1$ ,  $C_2$ , and  $C_3$ ). The parameter  $C_3$  can be selected such that a small  $\mathcal{M}$  is attained while maintaining a large  $C_2$ , which increases the speed of convergence. Thus, we conclude that dependency between the convergence speed and steady-state misadjustment exists [32]. Due to this reason, the variable step-size LMS algorithm employed in ADALINE converges prematurely during some critical conditions of estimation such as the presence of time-varying parameters, decaying DC function, high-level measurement noise and inter-harmonics in the signal. As a result, the algorithm needs large time for convergence and the accuracy of the estimation gets diminished.

**C. STABILITY ANALYSIS**

To ensure the stability of the DSSLMS algorithm,  $\mu_i(n)$  must be bounded within a certain positive range that yields the following condition.

$$0 < \mu_{min} \leq \mu_i(n) \leq \mu_{max} < 2/3tr[R] \tag{12}$$

where  $\mu_{min}$  is selected to be a very small value and  $\mu_{max}$  is chosen to be very close to the upper bound  $2/3tr[R]$ . The range between  $\mu_{min}$  and  $\mu_{max}$  plays a role in stability for such time-varying step-size.

The required computational resources of ADALINE with DSSLMS weight adaptation rule is  $(2L + 7)$  numbers of matrix multiplications/divisions and  $(2L + 3)$  numbers of

matrix additions/subtractions for performing a single iteration [21]. In addition, this algorithm necessarily needs  $(2L + 12)$  memory locations to store the signal samples, coefficients and variable parameters.

**III. ARCHITECTURE OF PROPOSED MASTER SLAVE ADALINE STRUCTURE**

To eliminate the tradeoff between the speed of convergence and steady-state misadjustment, and simultaneously accelerate the convergence rate in the above critical situations, the authors have proposed a novel two-fold parallel architecture named MS ADALINE. Fig. 2. illustrates the functional block diagram of MS ADALINE for parameter estimation. This recommended architecture consists of two ADALINE i.e. Master-ADALINE and Slave-ADALINE, whose corresponding weights are denoted as  $\{\widehat{a}_{iM}(n), \widehat{b}_{iM}(n)\}_{i=1}^L$  and  $\{\widehat{a}_{iS}(n), \widehat{b}_{iS}(n)\}_{i=1}^L$ . The signals  $\{x_{ai}(n), x_{bi}(n)\}_{i=1}^L$  are represented as common reference inputs for both ADALINE. The error outputs  $e_M(n)$  and  $e_S(n)$  are collected from Master-ADALINE and Slave-ADALINE, subsequently. In this research work, the subscript ‘M’ stands for Master-ADALINE’s parameters, whereas subscript ‘S’ indicates the parameters associated with Slave-ADALINE. The Slave-ADALINE uses an LMS algorithm with a fixed and large step-size value  $\mu_{iS}$ , which makes the convergence faster. On the other hand, the Master-ADALINE follows a variable step-size parameter  $\mu_{iM}(n)$ , which is reinitialized by the decision controller circuit for producing a small steady-state error. At the end of each iteration, the sum of squared errors of both ADALINE is calculated and fed to the decision controller circuit. The decision controller circuit compares these magnitudes and updates the coefficients of Master-ADALINE accordingly. If the sum of squared error of Master-ADALINE is greater than the sum of squared error of Slave-ADALINE, it means that the performance of the Slave-ADALINE is much more superior to Master-ADALINE. Its weights approach towards the optimum value. In this situation, the Master-ADALINE has used the weights of the Slave-ADALINE. At the same time, the step-size is



increased from  $\mu_{iM}(n)$  to  $(\mu_{iM}(n) + \mu_{max})/2$ , which raise the speed of convergence of the Master-ADALINE. This case arises at the starting stages of estimation or transients when both adaptive filters are far from the optimum weights. After a number of iterations, Slave-ADALINE close to the steady-state and its sum of squared error will be larger than the sum of squared error of the Master-ADALINE. At the same time, the step-size of Master-ADALINE decrease from  $\mu_{iM}(n)$  to  $C_4\mu_{iM}(n)$ , in order to maintain a low steady-state misadjustment. Finally,  $\mu_{iM}(n)$  approaching to a minimum value  $\mu_{min}$  and the filter coefficients attain the wiener solution. So, the system can overcome the effect of large estimation error by using MS ADALINE technique. By utilizing the weights of the Master-ADALINE, the amplitudes and phases are estimated.

**A. PROPOSED WEIGHT UPDATING RULE**

The weights of the Master-ADALINE and Slave-ADALINE are updated by the following steps:

*Step-1: Calculate the control signal  $y_S(n)$  and the instantaneous error  $e_S(n)$  of the Slave-ADALINE.*

$$y_S(n) = \sum_{i=1}^L [\widehat{a}_{iS}(n) \quad \widehat{b}_{iS}(n)] \begin{bmatrix} x_{ai}(n) \\ x_{bi}(n) \end{bmatrix} \quad (13)$$

$$e_S(n) = i(n) - y_S(n) \quad (14)$$

*Step-2: Calculate the control signal  $y_M(n)$  and the instantaneous error  $e_M(n)$  of the Master-ADALINE.*

$$y_M(n) = \sum_{i=1}^L [\widehat{a}_{iM}(n) \quad \widehat{b}_{iM}(n)] \begin{bmatrix} x_{ai}(n) \\ x_{bi}(n) \end{bmatrix} \quad (15)$$

$$e_M(n) = i(n) - y_M(n) \quad (16)$$

*Step-3: Update the Fourier coefficients  $\{\widehat{a}_{iS}(n), \widehat{b}_{iS}(n)\}_{i=1}^L$  of the Slave-ADALINE.*

$$\begin{aligned} \widehat{a}_{iS}(n+1) &= \widehat{a}_{iS}(n) + \mu_{iS}e_S(n)x_{ai}(n) \\ \widehat{b}_{iS}(n+1) &= \widehat{b}_{iS}(n) + \mu_{iS}e_S(n)x_{bi}(n) \end{aligned} \quad (17)$$

*Step-4: Compute the local averages of the square errors  $\{A_S(m), A_M(m)\}$  of both ADALINE.*

$$A_S(m) = \sum_{m=n-Q-1}^n e_S^2(m), \quad \text{for } n = Q, 2Q, 3Q \dots \quad (18)$$

$$A_M(m) = \sum_{m=n-Q-1}^n e_M^2(m), \quad \text{for } n = Q, 2Q, 3Q \dots \quad (19)$$

where  $Q$  is the length of the test interval that controls the convergence rate of the Master-ADALINE. If  $Q$  is assumed to be too large then the adaptation of the step-size of the Master-ADALINE is lost. However, if  $Q$  is too small, the step-size  $\mu_{iM}(n)$  will have large variations in the steady-state. For large values of  $Q$ , the Slave-ADALINE might converge inside the test interval and  $\mu_{iM}(n)$  is not sufficiently increased. In this situation, the convergence rate will be very slow. Here the value of  $Q$  is chosen as 50 for obtaining a satisfactory result.

*Step-5: Update the Fourier Coefficients  $\{\widehat{a}_{iM}(n), \widehat{b}_{iM}(n)\}_{i=1}^L$  of the Master-ADALINE.*

$$\begin{aligned} \widehat{a}_{iM}(n+1) &= \begin{cases} \widehat{a}_{iM}(n+1), & \text{if } A_S(m) < A_M(m) \\ \widehat{a}_{iM}(n) + \mu_{iM}(n)e_M(n)x_{ai}(n), & \text{else} \end{cases} \\ \widehat{b}_{iM}(n+1) &= \begin{cases} \widehat{b}_{iM}(n+1), & \text{if } A_S(m) < A_M(m) \\ \widehat{b}_{iM}(n) + \mu_{iM}(n)e_M(n)x_{bi}(n), & \text{else} \end{cases} \end{aligned} \quad (20)$$

*Step-6: Reinitialize the step-size parameter  $\mu_{iM}(n)$  of the Master-ADALINE.*

$$\mu_{iM}(n+1) = \begin{cases} \frac{(\mu_{iM}(n) + \mu_{max})}{2}, & \text{if } A_S(m) < A_M(m) \\ \max[C_4\mu_{iM}(n), \mu_{min}], & \text{else} \end{cases} \quad (21)$$

where  $(0 < C_4 < 1)$  is the scaling factor that regulates the adaptation of step-size and convergence rate. If  $C_4 \simeq 0$ , then the value of  $\mu_{iM}(n)$  is reduced too fast and the convergence of the algorithm is diminished. When  $C_4 \simeq 1$ , the algorithm will have poor convergence rate. By trial and error method, the authors chose the typical value for  $C_4$  is 0.9.

*Step-7: Estimate the amplitudes  $\{I_i\}_{i=1}^L$  and phases  $\{\Phi_i\}_{i=1}^L$  from Master-ADALINE coefficients.*

$$I_i(n) = \sqrt{\widehat{a}_{iM}^2(n) + \widehat{b}_{iM}^2(n)} \quad (22)$$

$$\Phi_i(n) = \tan^{-1}(\widehat{b}_{iM}(n)/\widehat{a}_{iM}(n)) \quad (23)$$

*Step-8: Calculate the MSE of Slave-ADALINE  $J_S(n)$  and Master-ADALINE  $J_M(n)$ .*

The MSE of Slave-ADALINE  $J_S(n)$  and Master-ADALINE  $J_M(n)$  can be obtained as

$$J_S(n) = J_{opt} + tr[RK_S(n)] \quad (24)$$

$$J_M(n) = J_{opt} + tr[RK_M(n)] \quad (25)$$

where  $J_{opt}$  is the optimal MSE, which can be expressed as  $J_{opt} = \lim_{n \rightarrow \infty} E\{e_{opt}^2(n)\}$ . The value of  $J_{opt}$  for both filters is equal. The correlation matrixes of the weight-error vector  $V_S(n)$  and  $V_M(n)$  are expressed as  $K_S(n) = E[V_S(n)V_S^T(n)]$  and  $K_M(n) = E[V_M(n)V_M^T(n)]$ . Referring [32], [33], the MSE of the LMS with fixed step-size is written as

$$J(n) = J_{opt} + \sum_{j=1}^N \lambda_j (1 - \mu\lambda_j)^2 v_j^2(0) \quad (26)$$

where  $\lambda_j$  is the  $j^{th}$  eigenvalue of the input autocorrelation matrix,  $v_j(0)$  is the  $j^{th}$  element of the vector  $V(0)$ . Taking into account that during one test interval the step-sizes of both ADALINE are constant, the MSE equations can be obtained from Eq. 26 as

$$\begin{aligned} J_S(kT) &= J_{opt} + \sum_{j=1}^N \lambda_j (1 - \mu_S\lambda_j)^{2T} v_{Sj}^2((k-1)T) \end{aligned} \quad (27)$$

$$\begin{aligned} J_M(kT) &= J_{opt} + \sum_{j=1}^N \lambda_j (1 - \mu_M((k-1)T)\lambda_j)^{2T} v_{Mj}^2((k-1)T) \end{aligned} \quad (28)$$

where  $T$  is the number of iterations and  $k$  is an integer. We assume that at the starting point of the test interval the Master-ADALINE weights are re-initialized with Slave-ADALINE, therefore we have

$$v_{Sj}((k - 1) T) = v_{Mj}((k - 1) T) \quad (29)$$

Eq. 27 to Eq. 29, it is clear that MSE of the Slave-ADALINE is smaller than the MSE of the Master-ADALINE at the final point of the test interval. This evaluation was made for a test interval ( $n$  from  $(k - 1)T$  to  $kT$ ) with the assumption that the coefficients  $[\widehat{a}_{iM}(n) \widehat{b}_{iM}(n)]$  are initialized with  $[\widehat{a}_{iS}(n) \widehat{b}_{iS}(n)]$  at  $n = (k - 1)T$ . The MSE of both ADALINE, at time instant  $n = kT$  can be approximated by

$$J_S(kT) = J_{opt} + \sum_{j=1}^N \lambda_j (1 - \mu_S \lambda_j)^{2T} v_{Sj}((k - 2) T) \quad (30)$$

$$J_M(kT) = J_{opt} + \sum_{j=1}^N \lambda_j (1 - \mu_M((k - 1) T) \lambda_j)^T \times (1 - \mu_M((k - 2) T) \lambda_j)^T v_{Mj}^2((k - 2) T) \quad (31)$$

It is concluded that the Slave-ADALINE has a smaller level of MSE than Master-ADALINE. At the steady-state condition, the MSE of Slave-ADALINE  $J_S(n)$  can be approximated as

$$J_S(n) = J_{opt} + J_{opt} \frac{\mu_{max}}{2} tr[R] \quad (32)$$

Since the Slave-ADALINE converges faster than the Master-ADALINE, the step-size  $\mu_{iM}(n)$  will only be reduced after Slave-ADALINE is converged. Finally,  $\mu_{iM}(n)$  attains its minimum bound  $\mu_{min}$ , the Master-ADALINE converges to the following level of MSE.

$$J_M(n) = J_{opt} + J_{opt} \frac{\mu_{min}}{2} tr[R] \quad (33)$$

The proposed algorithm is summarized as the Slave-ADALINE dominates the adaptive process at the training interval or transients, while the Master-ADALINE takes over during the last process. Their sum of squared errors at a specific adaptive interval is selected as the transfer criteria.

### B. MISADJUSTMENT LEVEL

For a stationary environment, the steady-state misadjustment of the Slave-ADALINE is approximately

$$\mathcal{M} = \frac{\mu_{iS}}{2} tr[R] \quad (34)$$

At the steady-state condition, the step-size of the Master-ADALINE  $\mu_{iM}(n)$  converges to  $\mu_{min}$ , then the misadjustment is given by

$$\mathcal{M} = \frac{\mu_{min}}{2} tr[R] \quad (35)$$

Eq. 34 and Eq. 35, it is noted that the steady-state misadjustment is independent of convergence speed. Therefore, the algorithm needs less time for convergence and the accuracy of the estimation becomes more exact.

### C. STABILITY ANALYSIS

In the Slave-ADALINE, the fixed step-size  $\mu_{iS}$  could be large as long as stable convergence is maintained. A necessary and sufficient condition for the mean square bounded weights is that

$$0 < \mu_{min} \ll \mu_{iS} \leq \mu_{max} < 2/3tr[R] \quad (36)$$

The stability, as well as the learning behaviour of the Master-ADALINE, is guaranteed if we bound the time-varying step-size  $\mu_{iM}(n)$  [31]. According to

$$0 < \mu_{min} \leq \mu_{iM}(n) \leq \mu_{max} < 2/3tr[R] \quad (37)$$

The MS ADALINE requires  $(4L + 6)$  numbers of matrix multiplications/divisions and  $(4L + 3)$  numbers of matrix additions/subtractions per iteration. The computational cost of the proposed architecture is effectively higher than the conventional architecture due to the use of twice number addition and multiplication blocks. The memory loads of the MS ADALINE are  $(3L + 14)$ .

In this work, the authors have further implemented three-fold or higher version architectures for harmonic estimation. But, it is observed that there is no such type of advantages over the proposed two-fold architecture except convergence speed. If the extra number of ADALINES is preferred, then the required computational resources are effectively increased that undoubtedly inflation of cost. This type of complexity architectures demoralizes for its practical implementation. However, the steady-state MSE functions of each ADALINE are nonlinear in nature, so their calculations are very much complicated. In addition, optimum step-size is required for minimizing the MSE. But, the calculation of optimum step-size necessary requires many assumptions of system parameters. Furthermore, the dependency between the steady-state misadjustment and convergence speed exists like single fold ADALINE with DSSLMS algorithm. Due to the above reasons, the three-fold architecture or even more is not an uncomplicated and cost-effective solution for harmonic parameter estimation.

### IV. SIMULATION RESULTS

Comprehensive simulation is carried out using MATLAB to verify the effectiveness of the proposed MS ADALINE approach for power system harmonic estimation. The current signal considered for the simulation is composed of odd harmonics of 3<sup>rd</sup>, 5<sup>th</sup>, 7<sup>th</sup>, 9<sup>th</sup>, 11<sup>th</sup>, 13<sup>th</sup> and 15<sup>th</sup> apart from the fundamental. The expression of an assumed signal is described as follows.

$$i(t) = 10.17 \sin(\omega t + 17.8^\circ) + 2.02 \sin(3\omega t - 16.8^\circ) + 1.62 \sin(5\omega t + 26.2^\circ) + 0.89 \sin(7\omega t + 58.4^\circ) + 0.75 \sin(9\omega t - 87.2^\circ) + 0.58 \sin(11\omega t + 60.1^\circ) + 0.4 \sin(13\omega t + 50^\circ) + 0.13 \sin(15\omega t + 39.5^\circ) + Nrand(t) \quad (38)$$

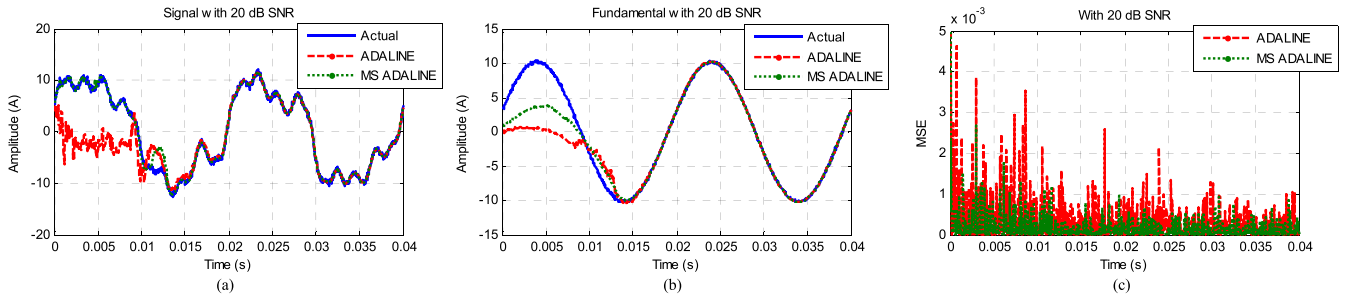


FIGURE 3. Estimated waveforms under 20 dB Noise condition. (a) Test signal. (b) Fundamental component. (c) MSE.

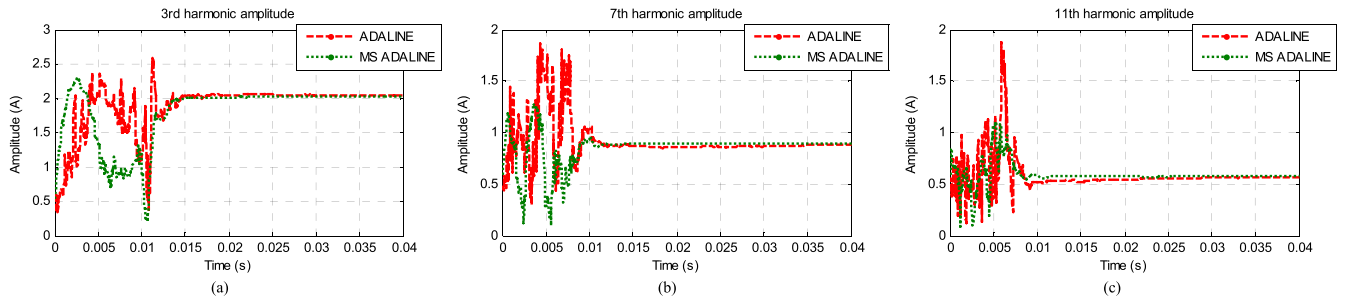


FIGURE 4. Estimated amplitudes under 20 dB Noise condition. (a) 3<sup>rd</sup>. (b) 7<sup>th</sup>. (c) 11<sup>th</sup>.

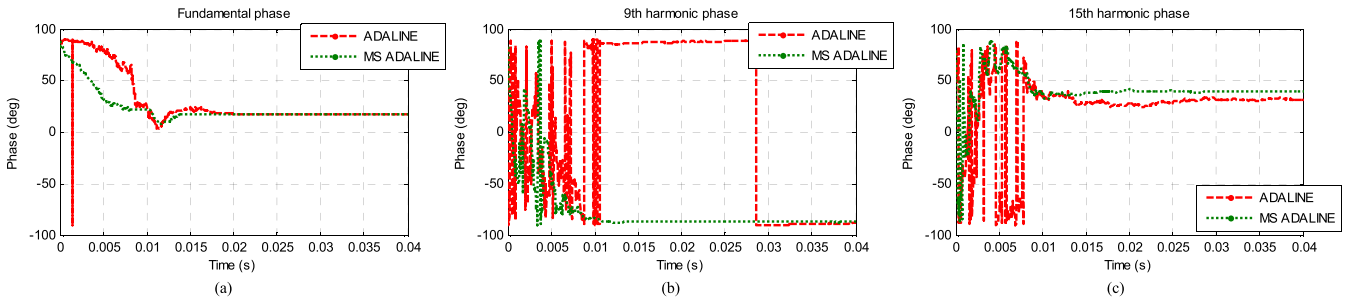


FIGURE 5. Estimated phases under 20 dB Noise condition. (a) Fundamental. (b) 9<sup>th</sup>. (c) 15<sup>th</sup>.

Simulation results are analysed with different sets of Gaussian noise of zero mean such as no noise, 20 dB SNR and 5 dB SNR corresponding to  $N = 0, 0.1$  and  $0.562$  (assuming  $S = 1$  for all sets). Signal to noise ratio (SNR) is defined as the logarithmic ratio of the signal and noise, i.e.  $SNR_{dB} = 20 \log_{10}(S/N)$ . The supply and sampling frequencies are considered as 50 Hz and 10 kHz, respectively. Table 1 summarizes the values of the various constants selected for the simulations of the two different adaptive techniques.

**A. ESTIMATION OF SIGNALS WITH DIFFERENT SNR**

Fig. 3(a)-(c) illustrates the estimated test signal, fundamental component, MSE using two different techniques at 20 dB SNR. From these figures, it is noticed that extremely accurate estimation is achieved by employing the proposed MS ADALINE method. However, the conventional ADALINE method shows more irregularity and oscillation in the first cycle based on 50 Hz fundamental waveform.

TABLE 1. Values of the constants parameters.

Parameters	ADALINE with DSSLMS algorithm	MS ADALINE with fixed and variable step sizes
Constants	$C_1 = 0.97, C_2 = 0.013, C_3 = 0.99$ [8], [30]	$C_4 = 0.9, Q = 50$
Coefficients	$\hat{a}_i(0) = \hat{b}_i(0) = 0.018$ [9], [21]	$\hat{a}_{iM}(0) = \hat{b}_{iM}(0) = 0.018, \hat{a}_{iS}(0) = \hat{b}_{iS}(0) = 0.018$
Step-size	$\mu_{max} = 0.008, \mu_{min} = 10^{-4}, \mu_i(0) = \mu_{max}$ [9], [31]	$\mu_{max} = 0.008, \mu_{min} = 10^{-4}, \mu_{iM}(0) = \mu_{min}, \mu_{iS} = \mu_{max}$

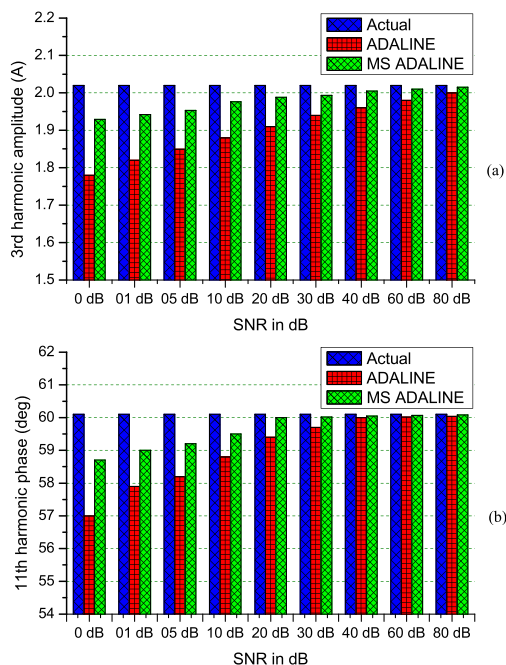
**B. ESTIMATION OF STEADY STATE PARAMETER**

Fig. 4 and 5 illustrate the corresponding amplitude and phase estimation of fundamental as well as other individual harmonic components present in the current signal added with random noise of 20 dB SNR. It is evident from Fig 4(a) and

Fig 5(a) that estimation based on ADALINE technique tracks the actual value almost a fundamental period (i.e. 0.02 s) while considering the lower order harmonics. But, when we deal with the higher-order harmonics the tracking performance is very much affected as shown in Fig 4(b) and (c), and Fig 5(b) and (c). However, these estimated values are slightly fluctuating in behaviour that degrades the power quality assessment. On the other hand, the results obtained from MS ADALINE are more accurate and zero oscillation. These estimated values follow the actual value by taking less than three-fourth of the fundamental period (i.e. 0.015 s). Especially, for phase estimation, these collected results are absolutely impressive.

**C. ESTIMATION UNDER DIFFERENT NOISE CONDITIONS**

Fig. 6(a) and (b) emphasizes the comparison of robustness in estimating the 3<sup>rd</sup> harmonic amplitude and 11<sup>th</sup> harmonic phase with the variety of noise level (i.e. 0dB ≤ SNR ≤ 80dB), respectively. The results reveal that at 80 dB SNR, the accuracies for estimation employing both the techniques are very high and nearly equal. But with the decrease in SNR value (i.e. with the increase in noise level), the MS ADALINE based estimation performs better, and less variation between actual and estimated values as compared to ADALINE.



**FIGURE 6. Steady state performance comparison with different SNR. (a) 3<sup>rd</sup> harmonic amplitude. (b) 11<sup>th</sup> harmonic phase.**

**D. ESTIMATION IN THE PRESENCE OF SUB- AND INTER-HARMONICS**

Inter-harmonics are the non-integer multiples of the fundamental frequency. Sub-harmonics are treated as inter-harmonics when the frequencies are less than the fundamental frequency [13], [21]. In order to assess the performance of

the proposed MS ADALINE structure for harmonic estimation, a sub-harmonic component of 30 Hz frequency and an inter-harmonic component of 185 Hz frequency are considered along with the test signal. Now, we can represent this distorted waveform as

$$i_1(t) = 0.47\sin(0.6\omega t + 23.4^0) + 1.32\sin(3.7\omega t + 39.5^0) + i(t) \quad (39)$$

For assessment of parameters present in a distorted signal, the reference signals  $\{x_{aK}(n) = \sin(K\omega n), x_{bK}(n) = \cos(K\omega n)\}$  apply to the MS ADALINE structure as primary inputs; where  $K = 0.6$  and  $3.7$  for sub-harmonic and inter-harmonic components respectively. The estimated coefficients of Master-ADALINE and Slave-ADALINE are  $\{\widehat{a}_{KM}(n), \widehat{b}_{KM}(n)\}$  and  $\{\widehat{a}_{KS}(n), \widehat{b}_{KS}(n)\}$  respectively as shown in Fig. 7. In this figure, the authors displayed common inputs for sub- and inter-harmonic components. But in simulation, we have considered two separate inputs for corresponding parameter estimation.

Fig. 8(a)-(d) show the estimation of amplitude and phase of sub- and inter-harmonic components present in the test signal. The waveforms justify the superior performance of MS ADALINE in affording a better accuracy even with the signal containing 20 dB SNR. The estimated value based on ADALINE maintains a steady-state reference value by taking more than 0.02 s, whereas estimation employing MS ADALINE attains the same value within 0.015 s or less.

**E. ESTIMATION IN THE PRESENCE OF DECAYING DC COMPONENTS**

The existence of decaying DC components causes the power system distorted. This signal is non-periodic in nature, so the exact estimation of its parameter is a challenging task. The test signal  $i_2(t)$  embedded with decaying DC component can be represented as

$$i_2(t) = i(t) + Ae^{(-Bt)} \quad (40)$$

where  $A$  and  $1/B$  are the magnitude and time constant of the DC decaying offset respectively. Referring [13], [21], for parameter estimation, the reference inputs are  $\{x_a(n) = 1, x_b(n) = n\}$  and the corresponding coefficients for Master- and Slave-ADALINE are  $\{\widehat{a}_M(n), \widehat{b}_M(n)\}$  and  $\{\widehat{a}_S(n), \widehat{b}_S(n)\}$ , respectively. After a number of iterations, the decaying DC parameters can be computed as

$$A = \widehat{a}_M(n) \quad \text{and} \quad B = \widehat{b}_M(n)/\widehat{a}_M(n) \quad (41)$$

In this test,  $A = 1.78$  A and  $B = 1.59s^{-1}$  are chosen. The estimated parameters of the decaying DC function for SNR of 20 dB are shown in Fig. 8(e) and (f). It is observed that the estimation of decaying parameter employing MS ADALINE is very much accurate and the required convergence time is 0.012 s. Whereas the estimation utilizing ADALINE needs 0.02 s and 0.1 s to track  $A$  and  $B$ , respectively. Furthermore, these estimated values employing ADALINE are not so much accurate and marginally fluctuating in behaviour.



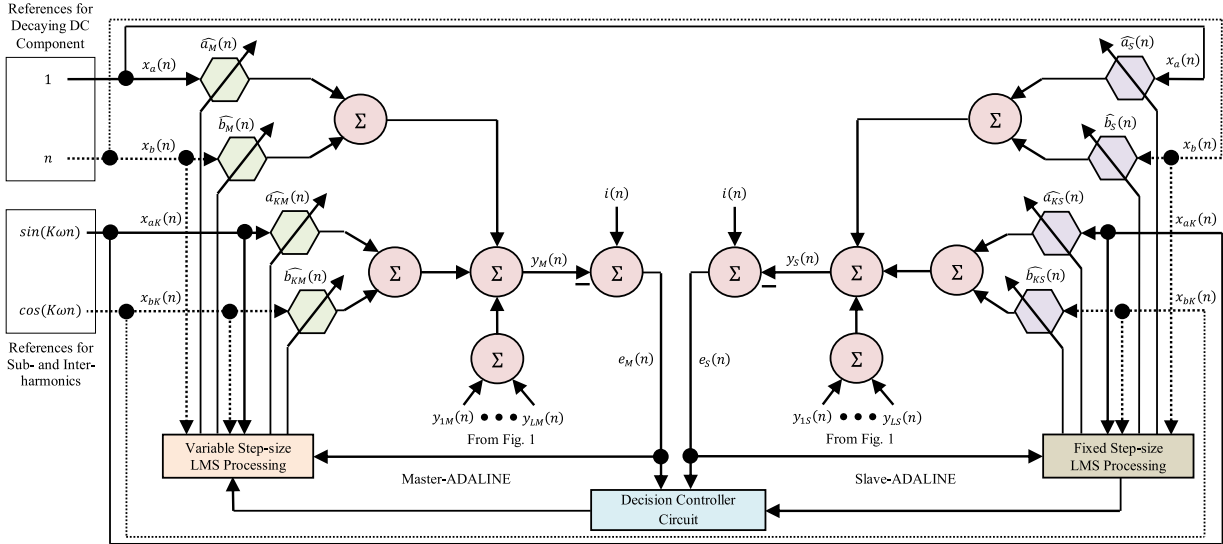


FIGURE 7. Block diagram of sub-harmonic, inter-harmonic and decaying DC components estimation.

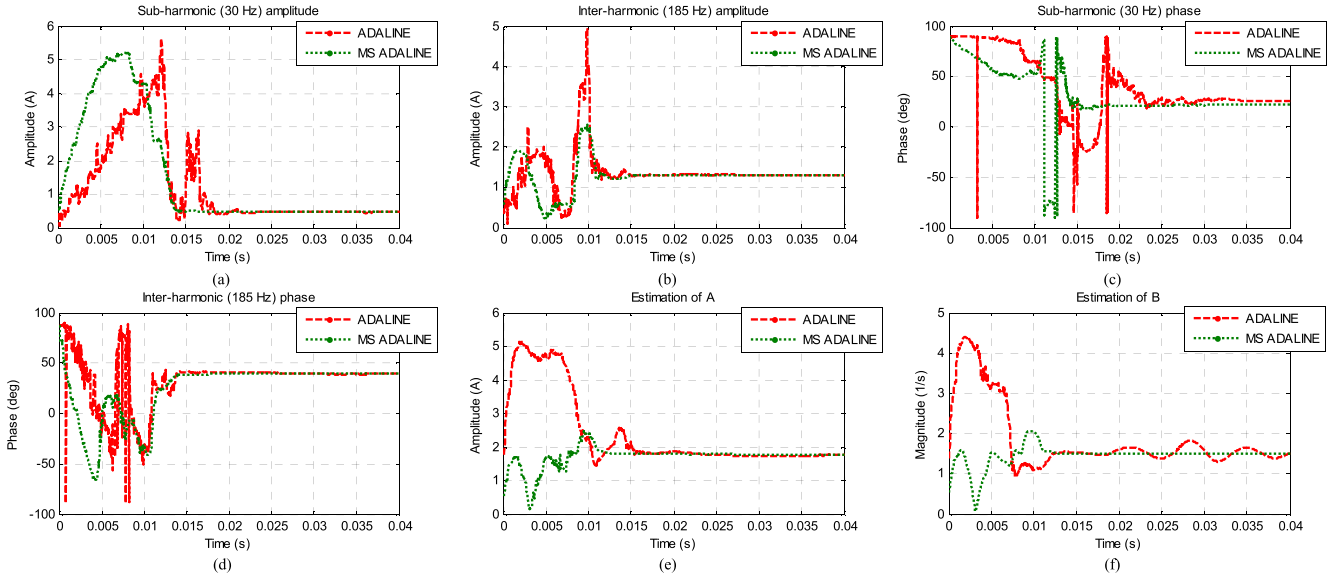


FIGURE 8. Estimated parameter at 20 dB SNR. (a) Sub-harmonic amplitude. (b) Inter-harmonic amplitude. (c) Sub-harmonic phase. (d) Inter-harmonic phase. (e) Decaying DC Magnitude. (f) Decaying DC time constant.

**F. ESTIMATION IN THE PRESENCE OF DYNAMIC SIGNAL**

To verify the performance of the MS ADALINE in transients, a time-varying 3<sup>rd</sup> harmonic amplitude is introduced in the test signal. In this study, the considered signal can be represented as

$$\begin{aligned}
 i_3(t) = & 10.17 \sin(\omega t + 17.8^0) \\
 & + (1.2 + i_d) \sin(3\omega t - 16.8^0) \\
 & + 1.62 \sin(5\omega t + 26.2^0) + 0.89 \sin(7\omega t + 58.4^0) \\
 & + 0.75 \sin(9\omega t - 87.2^0) + 0.58 \sin(11\omega t + 60.1^0) \\
 & + 0.40 \sin(13\omega t + 50^0) + 0.13 \sin(15\omega t + 39.5^0) \\
 & + 0.1rand(t)
 \end{aligned} \tag{42}$$

where  $i_d$  is the 3<sup>rd</sup> harmonic amplitude modulating parameter, it can be defined as

$$i_d = 0.96 \sin 0.02\omega t + 0.14 \sin 0.12\omega t \tag{43}$$

The estimation of time-varying 3<sup>rd</sup> harmonic amplitude in the presence of random noise is depicted in Fig. 9(a). It is observed that the estimation based on the ADALINE technique produces a vast amplitude deviation along with the poor convergence speed. However, by implementing the MS ADALINE technique, the convergence speed is found to be faster, calculated data became more accurate and percentage error is limited.

**G. ESTIMATION OF TIME VARYING PARAMETER**

The estimation of 5<sup>th</sup> order amplitude and 7<sup>th</sup> order phase under sudden step change from 1.82 A to 1.62 A and 20<sup>0</sup>

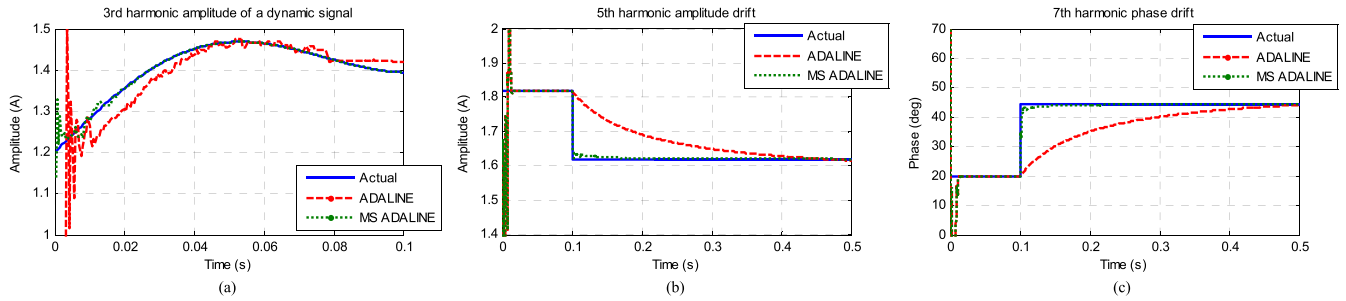


**FIGURE 9.** Estimation during transients at 20 dB SNR. (a) Time-varying 3<sup>rd</sup> harmonic amplitude. (b) 5<sup>th</sup> harmonic amplitude drift. (c) 7<sup>th</sup> harmonic phase drift.

**TABLE 2.** Percentage of amplitude error in different architectures.

Sl No	Estimation Methods	Parameters	Sub	Fund	3 <sup>rd</sup>	Inter	5 <sup>th</sup>	7 <sup>th</sup>	9 <sup>th</sup>	11 <sup>th</sup>	13 <sup>th</sup>	15 <sup>th</sup>
		Freq (Hz)	30	50	150	185	250	350	450	550	650	750
		Amplitude	0.47	10.17	2.02	1.32	1.62	0.89	0.75	0.58	0.40	0.13
1	ADALINE with fixed step-size LMS ( $\mu_i = \mu_{max}$ )	Amplitude	0.418	9.02	1.84	1.23	1.49	0.82	0.696	0.54	0.377	0.122
		Error (%)	11.06	11.3	8.91	6.81	8.02	7.86	7.2	6.89	5.75	6.15
2	ADALINE with fixed step-size LMS ( $\mu_i = \mu_{min}$ )	Amplitude	0.424	9.15	1.88	1.25	1.53	0.845	0.707	0.549	0.382	0.123
		Error (%)	9.78	10.02	6.93	5.30	5.55	5.05	5.73	5.34	4.5	5.38
3	ADALINE with DSSLMS (Conventional Method)	Amplitude	0.434	9.377	1.92	1.26	1.569	0.864	0.713	0.562	0.394	0.124
		Error (%)	7.65	7.79	4.95	4.54	3.14	2.92	4.93	3.10	1.5	4.61
4	Hybrid FFT-ADALINE [18]	Amplitude	0.44	9.593	1.94	1.277	1.56	0.869	0.723	0.566	0.395	0.126
		Error (%)	6.38	5.67	3.96	3.25	3.84	2.35	3.6	2.41	1.25	3.07
5	Gauss-Newton ADALINE [23]	Amplitude	0.447	9.67	1.96	1.297	1.571	0.872	0.73	0.567	0.396	0.127
		Error (%)	4.89	4.91	2.97	1.74	3.02	2.02	2.66	2.24	1.00	2.30
6	MS ADALINE (Proposed Method)	Amplitude	0.459	9.777	1.995	1.31	1.59	0.88	0.736	0.571	0.398	0.128
		Error (%)	2.34	3.86	1.23	0.75	1.85	1.12	1.86	1.55	0.5	1.53

to 50<sup>0</sup> at  $t = 0.1$  s are illustrated in Fig. 9(b) and (c), respectively. It is observed from the waveforms that estimation based on ADALINE lost its capability to track the sudden variations and chased the actual value within 0.4 s. However, the MS ADALINE based estimation precisely followed these changes with a minor delay of 0.05 s.

Finally, this study concluded that the tracking performances of both algorithms are approximately equal under steady-state without noise. But, steady-state with high noise level and critical conditions, the performance of MS ADALINE is much more superior to single-stage ADALINE.

**H. PERFORMANCE EVALUATION OF MS ADALINE COMPARING WITH OTHER RECENT ARCHITECTURE**

Table 2 and 3 exhibit the percentage error of corresponding amplitude and phase of fundamental, harmonics, inter-harmonic, sub-harmonic components using four different adaptive algorithms. The percentage of error can be calculated for  $N$  length of the estimated signal as

$$Error (\%) = \frac{1}{N} \sum_{n=1}^N \frac{|i(n) - y(n)|}{i(n)} \quad (44)$$

From Table 2, it is noticed that at 20 dB SNR the highest error occurs in the fundamental amplitude of 11.3%, 10.02%, 7.79%, 5.67%, 4.91%, and 3.86%, and the lowest error in the 13<sup>th</sup> harmonic amplitude of 5.75%, 4.5%, 1.50%, 1.25%, 1.00%, and 0.5%, by employing ADALINE with fixed and large step-size LMS algorithm (Design 1), fixed and small step-size LMS algorithm (Design 2), variable step-size LMS algorithm (Design 3), Hybrid FFT (Design 4) [18], Gauss-Newton (Design 5) [23], and MS ADALINE with both fixed and variable step-size LMS algorithm i.e. proposed technique (Design 6), subsequently. The phase estimation using the above six adaptive techniques are shown in Table 3, the corresponding highest error of 16.93%, 14.20%, 12.87%, 8.10%, 7.34%, and 3.58% arises in 15<sup>th</sup> harmonic and lowest error of 5.95%, 3.09%, 1.32%, 1.14%, 1.01%, and 0.23% achieve in 3<sup>rd</sup> harmonic. In Design 1, the convergence speed is very fast, but the steady-state error is large. In Design 2 the convergence speed is slow, but the steady-state error is small. Designs 3-5 is achieved a small steady-state error than the above two designs, but the interaction exists between the steady-state misadjustment and convergence speed degrade its performance. In Design 6, the step-size adaptation is

TABLE 3. Percentage of phase error in different architectures.

Sl No	Estimation Methods	Parameters	Sub	Fund	3 <sup>rd</sup>	Inter	5 <sup>th</sup>	7 <sup>th</sup>	9 <sup>th</sup>	11 <sup>th</sup>	13 <sup>th</sup>	15 <sup>th</sup>
		Freq (Hz)	30	50	150	185	250	350	450	550	650	750
		Phase	23.4	17.8	-16.8	39.5	26.2	58.4	-87.2	60.1	50	39.5
1	ADALINE with fixed step-size LMS ( $\mu_i = \mu_{max}$ )	Phase	20.57	16.6	-15.8	36.55	23.89	54.66	-80.7	56.06	47.02	32.81
		Error (%)	12.09	6.74	5.95	7.46	8.81	6.49	7.45	6.72	5.96	16.93
2	ADALINE with fixed step-size LMS ( $\mu_i = \mu_{min}$ )	Phase	21.03	16.9	-16.28	37.7	24.56	56.47	-82.6	58.01	48.2	33.89
		Error (%)	10.12	5.05	3.09	4.55	6.25	3.30	5.27	3.47	3.6	14.20
3	ADALINE with DSSLMS (Conventional Method)	Phase	21.738	17.111	-16.57	38.16	24.793	57.588	-83.33	58.771	48.71	34.416
		Error (%)	7.1	3.87	1.32	3.39	5.37	1.39	4.43	2.21	2.58	12.87
4	Hybrid FFT-ADALINE [18]	Phase	22.08	17.3	-16.607	38.6	25.57	57.6	-84.2	59.0	49.13	36.3
		Error (%)	5.64	2.80	1.14	2.28	2.40	1.36	3.44	1.83	1.74	8.10
5	Gauss-Newton ADALINE [23]	Phase	22.27	17.41	-16.63	38.71	25.79	57.63	-84.37	59.11	49.24	36.6
		Error (%)	4.82	2.19	1.01	2.00	1.56	1.33	3.24	1.64	1.52	7.34
6	MS ADALINE (Proposed Method)	Phase	22.75	17.64	-16.76	38.919	26.108	57.938	-85.91	59.511	49.59	38.085
		Error (%)	2.77	0.89	0.23	1.47	0.35	0.79	1.47	0.98	0.82	3.58

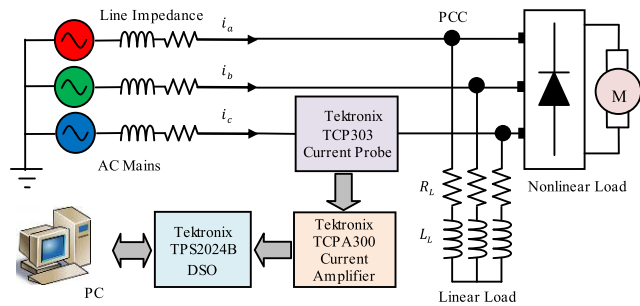


FIGURE 10. Line diagram of the test system for real time signal parameter estimation.

fully controlled by a decision controller circuit, where the steady-state misadjustment is independent of the rate of convergence. Therefore, Design 6 claims least percentage error among all four designs.

V. EXPERIMENTAL RESULTS

To demonstrate the comparative performance of proposed MS ADALINE over conventional ADALINE, a scaled laboratory prototype is developed. The experimental setup comprises of a thyristor bridge rectifier fed DC load acting as a non-linear load and another inductive load of the series combination of the inductance of rating 64.5 mH and resistance of 22.5Ω in each phase acting as a linear load. Both the loads are connected in parallel to the three-phase 415 V, 50 Hz source through an autotransformer and isolation transformer. This type of combinational load injects a huge amount of time-varying harmonics and impulsive noise into the system. Fig. 10 shows the line diagram of a test system and Fig. 11 depicts a photograph of the real experimental setup including other measuring instruments. Two Tektronix DMM4020 digital multimeters are used for accurate measurement of supply current and voltage up to three decimal

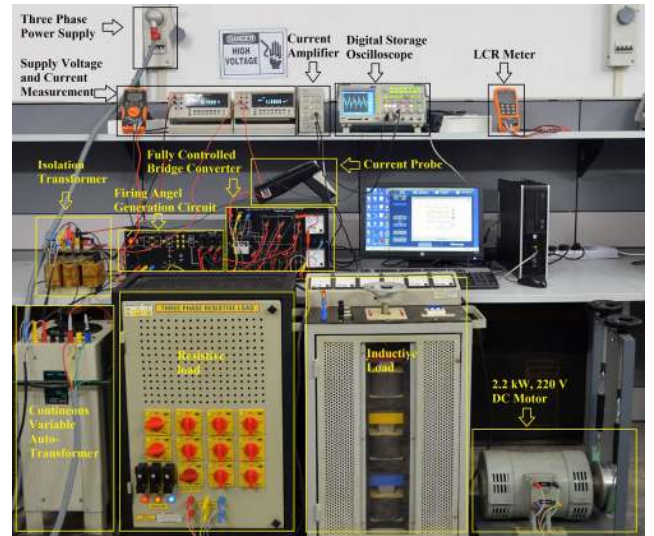
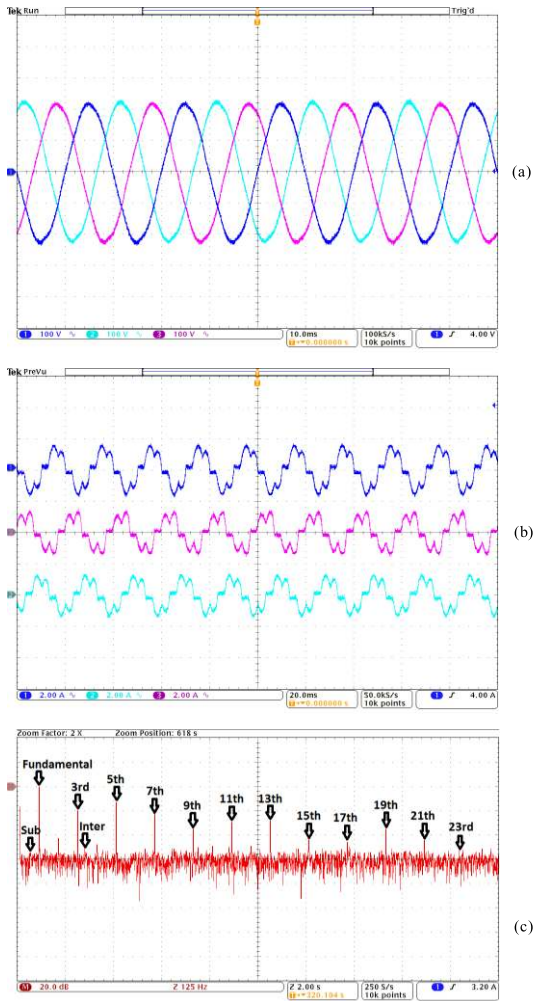


FIGURE 11. Photograph of the real experimental setup.

points. The current measurement system is comprised of Tektronix TCPA303 current probe for sensing the supply current and Tektronix TCPA300 current amplifier for proper amplification of the sensed current. Both supply current and voltage waveforms are collected online at the point of common coupling (PCC) and stored by using Tektronix TPS2024B digital storage oscilloscope (DSO) in the form of discrete data. The sampling frequency of the current probe, current amplifier and DSO are set to be 25 kHz. The DSO is interfaced with the HP desktop personal computer (PC) through DSO PC communication software. By using this software, the discrete data points are transferred to the PC. The measured signals are not filtered to avoid any phase lag due to filtering. The implementation is done via MATLAB R2019a on the PC. The collected instantaneous real-time discrete data has been



**FIGURE 12.** waveforms recorded by DSO. (a) Three phase supply voltages ( $X$  – axis =  $10ms/div$ ,  $Y$  – axis =  $100V/div$ ). (b) Three phase supply current ( $X$  – axis =  $10ms/div$ ,  $Y$  – axis =  $2A/div$ ). (c) Spectrum of phase-a supply current.

analyzed in the PC by implementing the proposed algorithm with the help of MATLAB. The measurement data is captured and analyzed on the PC after the experiments. The values of the constant parameters used for implementation are similar to simulated values.

The experimental waveforms of three-phase supply voltages, three-phase supply currents and phase-a supply current spectrum as recorded by the DSO are displayed in Fig. 12(a)-(c) respectively. From figures, it is observed that the supply voltages are almost sinusoidal. However, the supply currents are fully distorted because of the nonlinear load. This distorted current signal containing fundamental along with harmonics, sub-harmonics, inter-harmonics and additive noise, which is considered as a test signal for real-time analysis.

**A. ESTIMATED SIGNAL FROM REAL EXPERIMENTAL SETUP**

By using this real-time discrete data, the fundamental, the sum of harmonics up to 99<sup>th</sup> order and MSEs are

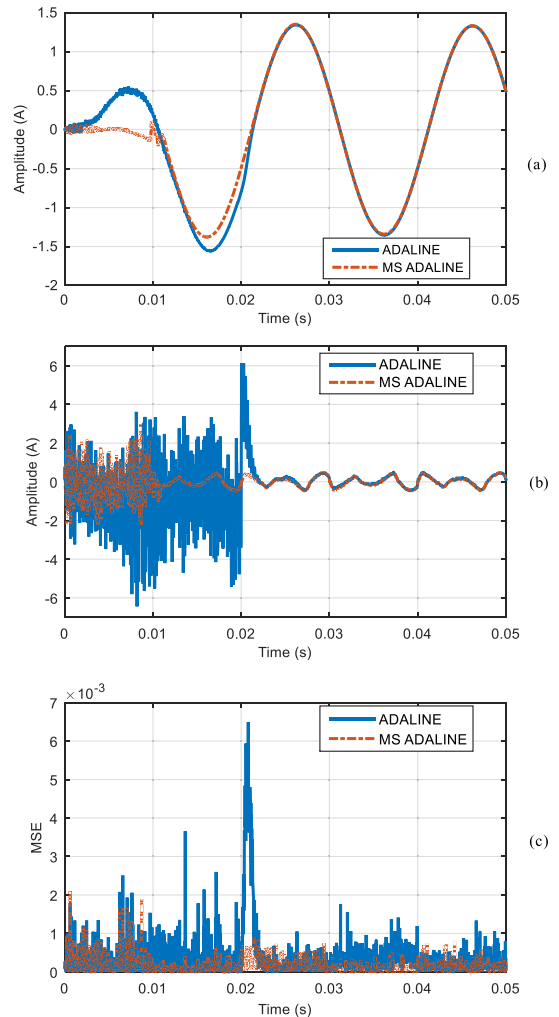


**FIGURE 13.** signals from the real time data. (a) Fundamental. (b) Sum of harmonics up to 99<sup>th</sup> order. (c) MSEs.

estimated as shown in Fig. 13(a)-(c), respectively. It is evident from these figures that the proposed algorithm completely filters out the additive noise as generated from the hardware and produces exact assessment results. The time point of convergence of MS ADALINE is approximately 0.01 s, which is same as the result obtained from the simulation study. However, estimation based on ADALINE suffers from huge oscillation before achieving the steady-state. This algorithm takes more than 0.02 s for settling down to the actual value. The magnitude of MSEs employing the proposed method is lower than the conventional method.

**B. ESTIMATED AMPLITUDES AND PHASES FROM REAL EXPERIMENTAL SETUP**

The estimation of amplitude of sub-harmonic, fundamental, inter-harmonic, 7<sup>th</sup>, 13<sup>th</sup>, 19<sup>th</sup> are illustrated in Fig. 14. Similarly, the estimated phase of sub-harmonic, fundamental, inter-harmonic, 5<sup>th</sup>, 11<sup>th</sup>, 17<sup>th</sup> are shown in Fig. 15. At  $t = 0^+$  s, the signal parameter shows transient



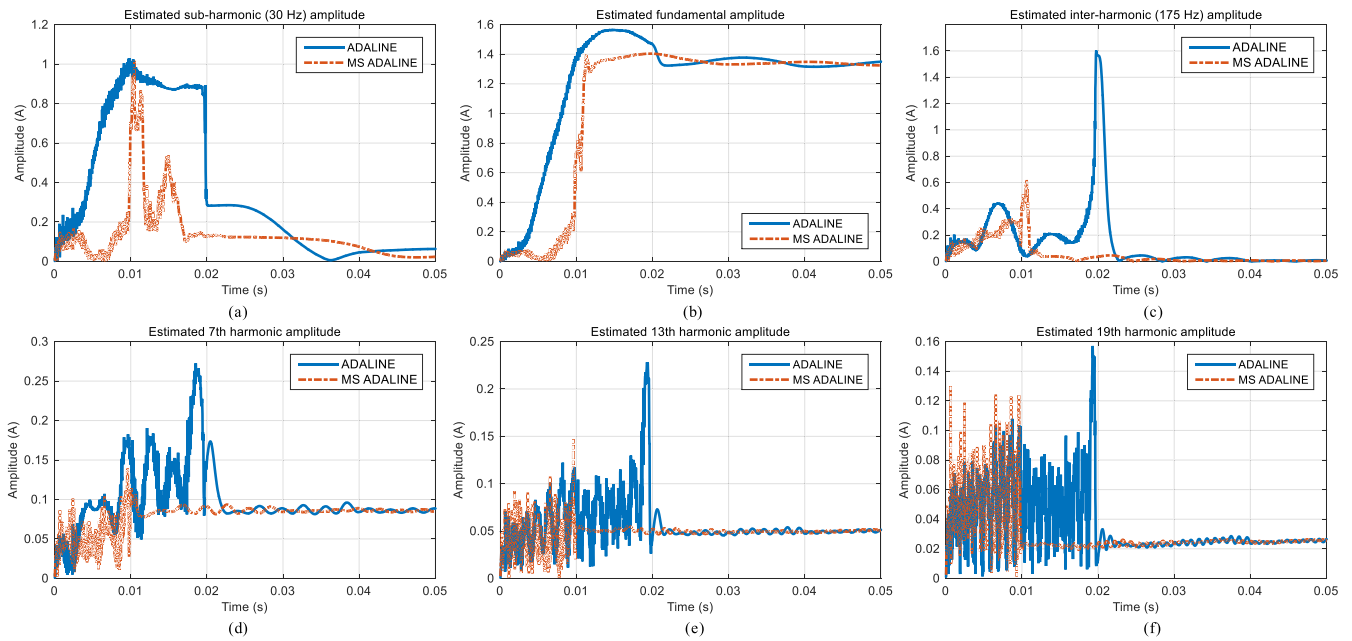


**FIGURE 14.** Estimated amplitudes from real experimental data. (a) Sub-harmonic of 30 Hz. (b) Fundamental. (c) Inter-harmonic of 175 Hz. (d) 7<sup>th</sup>. (e) 13<sup>th</sup>. (f) 19<sup>th</sup>.

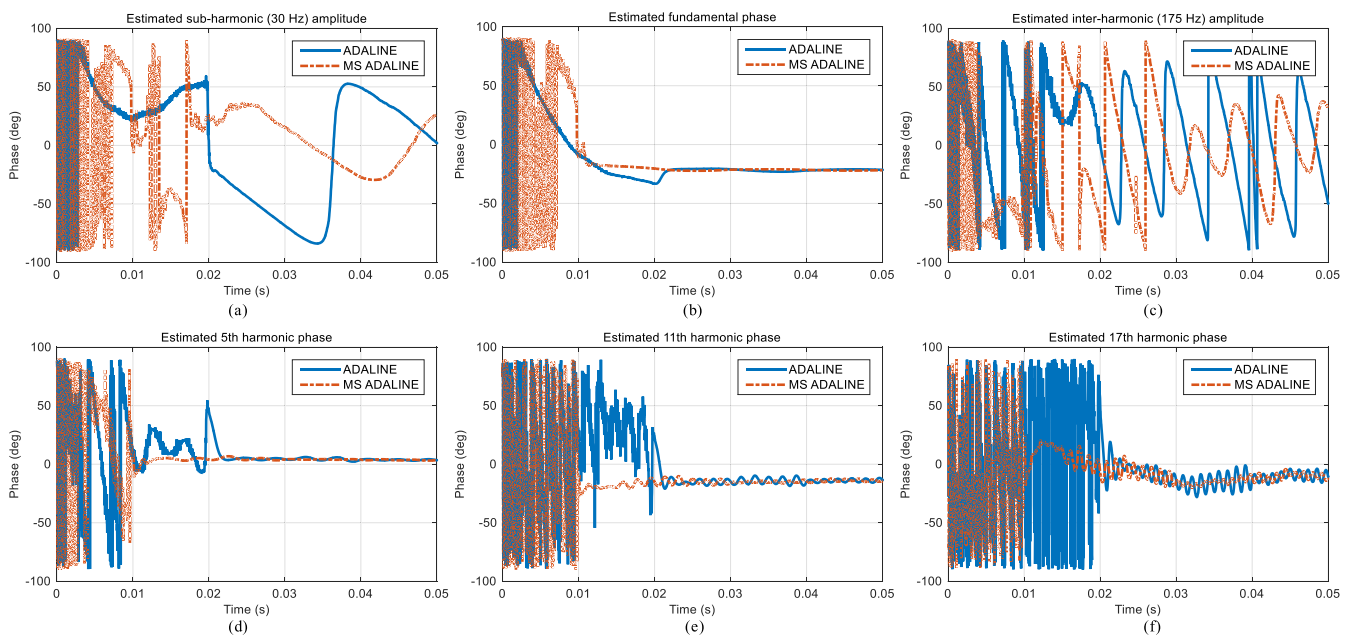


**FIGURE 15.** Estimated phases from real experimental data. (a) Sub-harmonic of 30 Hz. (b) Fundamental. (c) Inter-harmonic of 175 Hz. (d) 5<sup>th</sup>. (e) 11<sup>th</sup>. (f) 17<sup>th</sup>.

behaviour due to the initial interaction between the harmonic components. Therefore, for power quality assessment, the first two cycles are neglected. After the settling time, the system achieves a steady-state and parameter maintains a fixed value, then it is considered for estimation. It can be noticed from figures that MS ADALINE based approach approximately takes 250 iterations (i.e. 0.01 s) to track the actual

value of each harmonic component, whereas ADALINE technique requires more than 500 iterations (i.e. 0.02 s) to attain the same value. The required rate of convergence for MS ADALINE is around half of the ADALINE. By introducing the Slave-ADALINE along with the Master-ADALINE, the overall performance has been improved drastically under the real-time situation.

**TABLE 4. Settling time of different estimation algorithms.**

Sl No	Estimation Methods	Calculated Settling Time	
		Simulation Test	Experimental Test
1	ADALINE with DSSLMS (Conventional Method)	0.02 s	0.04 s
2	Hybrid FFT-ADALINE [18]	0.015 s	0.03 s
3	Gauss-Newton ADALINE [23]	0.015 s	0.03 s
4	MS ADALINE (Proposed Method)	0.01 s	0.01 s

## VI. CONCLUSION

In this work, a high-speed MS ADALINE technique is suggested for fast and exact measurement of the individual harmonic component in a distorted current signal. The steady-state performance employing the proposed technique is verified via MATLAB at various SNR values. It is evident from the simulation results that the highest amplitude and phase errors by applying MS ADALINE technique are 3.86% and 3.58%, respectively, whereas ADALINE based estimation provides the corresponding values of 7.79% and 12.87%. Moreover, the proposed structure is solid and robust against the presence of sub-harmonics, inter-harmonics, time-varying signals and decaying DC components. Subsequently, both techniques are implemented in the real-time environment. In order to validate the performance of the proposed structure, a comparison result between the simulation test and experimental test with same parameters and same scenarios are summarized in Table 4. It is observed that by employing recommended estimation theory, the simulated and experimental values of settling time are minimum and identical. The overall simulation and experimental results have demonstrated that the proposed estimation technique is admirable and powerful as compared to conventional ADALINE based estimation.

The future works of MS ADALINE are discussed in brief. For sustainable growth in the power system, recently renewable energy sources are gaining a lot of attention. These energy sources feeding power via power converters can be taken up as a further investigation in the field of power quality. This technique can be applied to the aircraft electrical power system for exact measurement of the harmonic content and thus the designing of dynamic filtering approach guarantees the power quality standards. By utilizing this technique simultaneously on load and source currents, we can evaluate the compensation effect of the active power filter (APF) system connected to the distribution power network.

## REFERENCES

- [1] C.-I. Chen and Y.-C. Chen, "Comparative study of harmonic and interharmonic estimation methods for stationary and time-varying signals," *IEEE Trans. Ind. Electron.*, vol. 61, no. 1, pp. 397–404, Jan. 2014.
- [2] V. K. Tiwari, A. C. Umarikar, and T. Jain, "Fast amplitude estimation of harmonics using undecimated wavelet packet transform and its hardware implementation," *IEEE Trans. Instrum. Meas.*, vol. 67, no. 1, pp. 65–77, Jan. 2018.
- [3] M. Bettayeb and U. Qidwai, "A hybrid least squares-GA-based algorithm for harmonic estimation," *IEEE Trans. Power Del.*, vol. 18, no. 2, pp. 377–382, Apr. 2003.
- [4] S. Mishra, "A hybrid least square-fuzzy bacterial foraging strategy for harmonic estimation," *IEEE Trans. Evol. Comput.*, vol. 9, no. 1, pp. 61–73, Feb. 2005.
- [5] A. Abdollahi and F. Matinfar, "Frequency estimation: A least-squares new approach," *IEEE Trans. Power Del.*, vol. 26, no. 2, pp. 790–798, Apr. 2011.
- [6] Z. Moravej and J. Enayati, "A hybrid least squares-clonal selection based algorithm for harmonics estimation," *Int. Trans. Electr. Energy Syst.*, vol. 24, no. 1, pp. 1–15, Jan. 2014.
- [7] M. Joorabian, S. S. Mortazavi, and A. A. Khayyami, "Harmonic estimation in a power system using a novel hybrid Least Squares-Adaline algorithm," *Electr. Power Syst. Res.*, vol. 79, no. 1, pp. 107–116, Jan. 2009.
- [8] A. K. Pradhan, A. Routray, and A. Basak, "Power system frequency estimation using least mean square technique," *IEEE Trans. Power Del.*, vol. 20, no. 3, pp. 1812–1816, Jul. 2005.
- [9] B. Subudhi, P. K. Ray, and S. Ghosh, "Variable leaky least mean-square algorithm-based power system frequency estimation," *IET Sci., Meas. Technol.*, vol. 6, no. 4, pp. 288–297, 2012.
- [10] M. Beza and M. Bongiorno, "Application of recursive least squares algorithm with variable forgetting factor for frequency component estimation in a generic input signal," *IEEE Trans. Ind. Appl.*, vol. 50, no. 2, pp. 1168–1176, Mar./Apr. 2014.
- [11] I. Sadinezhad and V. G. Agelidis, "Real-time power system phasors and harmonics estimation using a new decoupled recursive-least-squares technique for DSP implementation," *IEEE Trans. Ind. Electron.*, vol. 60, no. 6, pp. 2295–2308, Jun. 2013.
- [12] X. Nie, "Detection of grid voltage fundamental and harmonic components using Kalman filter based on dynamic tracking model," *IEEE Trans. Ind. Electron.*, vol. 67, no. 2, pp. 1191–1200, Feb. 2020.
- [13] P. K. Ray and B. Subudhi, "Ensemble-Kalman-filter-based power system harmonic estimation," *IEEE Trans. Instrum. Meas.*, vol. 61, no. 12, pp. 3216–3224, Dec. 2012.
- [14] C. Wu, M. E. Magana, and E. Cotilla-Sanchez, "Dynamic frequency and amplitude estimation for three-phase unbalanced power systems using the unscented Kalman filter," *IEEE Trans. Instrum. Meas.*, vol. 68, no. 9, pp. 3387–3395, Sep. 2019.
- [15] S. K. Jain and S. N. Singh, "Fast harmonic estimation of stationary and time-varying signals using EA-AWNN," *IEEE Trans. Instrum. Meas.*, vol. 62, no. 2, pp. 335–343, Feb. 2013.
- [16] D. O. Abdeslam, P. Wira, J. Merckle, D. Flieller, and Y.-A. Chapuis, "A unified artificial neural network architecture for active power filters," *IEEE Trans. Ind. Electron.*, vol. 54, no. 1, pp. 61–76, Feb. 2007.
- [17] M. Valtierra-Rodriguez, R. de Jesus Romero-Troncoso, R. A. Osornio-Rios, and A. Garcia-Perez, "Detection and classification of single and combined power quality disturbances using neural networks," *IEEE Trans. Ind. Electron.*, vol. 61, no. 5, pp. 2473–2482, May 2014.
- [18] Z. P. Goh, M. A. M. Radzi, Y. V. Thien, H. Hizam, and N. I. A. Wahab, "Hybrid FFT-ADALINE algorithm with fast estimation of harmonics in power system," *IET Signal Process.*, vol. 10, no. 8, pp. 855–864, Oct. 2016.
- [19] G. W. Chang, C.-I. Chen, and Q.-W. Liang, "A two-stage ADALINE for harmonics and interharmonics measurement," *IEEE Trans. Ind. Electron.*, vol. 56, no. 6, pp. 2220–2228, Jun. 2009.
- [20] A. Sarkar, S. R. Choudhury, and S. Sengupta, "A self-synchronized ADALINE network for on-line tracking of power system harmonics," *Measurement*, vol. 44, no. 4, pp. 784–790, May 2011.
- [21] P. Garanayak and G. Panda, "Fast and accurate measurement of harmonic parameters employing hybrid adaptive linear neural network and filtered-x least mean square algorithm," *IET Gener., Transmiss. Distrib.*, vol. 10, no. 2, pp. 421–436, Feb. 2016.
- [22] M. I. Marei, E. F. El-Saadany, and M. M. A. Salama, "A processing unit for symmetrical components and harmonics estimation based on a new adaptive linear combiner structure," *IEEE Trans. Power Del.*, vol. 19, no. 3, pp. 1245–1252, Jul. 2004.
- [23] S. Nanda and P. K. Dash, "A Gauss-Newton ADALINE for dynamic phasor estimation of power signals and its FPGA implementation," *IEEE Trans. Instrum. Meas.*, vol. 67, no. 1, pp. 45–56, Jan. 2018.
- [24] M. Qasim, P. Kanjiya, and V. Khadkikar, "Optimal current harmonic extractor based on unified ADALINEs for shunt active power filters," *IEEE Trans. Power Electron.*, vol. 29, no. 12, pp. 6383–6393, Dec. 2014.
- [25] B. Huang, Y. Xiao, Y. Ma, G. Wei, and J. Sun, "A simplified variable step-size LMS algorithm for Fourier analysis and its statistical properties," *Signal Process.*, vol. 117, pp. 69–81, Dec. 2015.

- [26] W. Huang, L. Li, Q. Li, and M. Yao, "Diffusion robust variable step-size LMS algorithm over distributed networks," *IEEE Signal Process. Mag.*, vol. 26, no. 3, pp. 81–93, May 2009.
- [27] D. Bismor, "Extension of LMS stability condition over a wide set of signals," *Int. J. Adapt. Control Signal Process.*, vol. 29, no. 5, pp. 653–670, May 2015.
- [28] H. Han, S. Zhang, and H. Liang, "Non-parametric variable step-size diffusion LMS algorithm over adaptive networks," *IEEE Access*, vol. 6, pp. 2169–3536, 2018.
- [29] S. Haykin, *Adaptive Filter Theory*. 4th ed. Englewood Cliffs, NJ, USA: Prentice-Hall, 2002.
- [30] J.-K. Hwang and Y.-P. Li, "Variable step-size LMS algorithm with a gradient-based weighted average," *IEEE Signal Process. Lett.*, vol. 16, no. 12, pp. 1043–1046, Dec. 2009.
- [31] T. Aboulnasr and K. Mayyas, "A robust variable step-size LMS-type algorithm: Analysis and simulations," *IEEE Trans. Signal Process.*, vol. 45, no. 3, pp. 631–639, Mar. 1997.
- [32] R. C. Bilcu, "On adaptive least mean square FIR filters: New implementations and applications," Ph.D. dissertation, Inst. Signal Process., Tampere Univ. Technol., Tampere, Finland, 2004.
- [33] B. F. Boroujeny, *Adaptive Filters: Theory and Applications*. 2nd ed. Toronto, ON, USA: Wiley, 1999.



**PRIYABRAT GARANAYAK** received the B.Tech. degree in electronics and telecommunication engineering from the Biju Patnaik University of Technology, India, in 2009, the M.Tech. degree with specialization in VLSI and embedded system design from the Centre for Micro Electronics, Biju Patnaik University of Technology, India, in 2011, and the Ph.D. degree from the Department of Electrical Engineering, National Institute of Technology at Meghalaya, India, in 2016.

From 2016 to 2017, he was a Project Assistant with the Electrical Engineering Department, IIT Delhi, India. He has worked as an Assistant Professor with the Department of Electronics and Communication Engineering, Indian Institute of Information Technology Pune, India, from 2017 to 2018. He has been with the Indian Institute of Information Technology Una, India, since 2018, where he is currently an Assistant Professor with the Electronics and Communication Engineering Department. His research interests are harmonic mitigation, harmonic estimation, active and hybrid filters, unified power quality conditioner (UPQC), adaptive signal processing applied to power systems, and renewable power generation.



**R. T. NAAYAGI** (Senior Member, IEEE) received the bachelor's degree (Hons.) in electrical and electronics engineering from Bharathidasan University, Tiruchirappalli, India, in 2000, the master's degree in information technology from Alagappa University, Karaikudi, India, in 2003, the master's degree (Hons.) in power electronics and drives from Anna University, Chennai, India, in 2005, and the Ph.D. degree in electrical and electronic engineering from The University of Manchester, Manchester, U.K., in 2010.

She held various roles as a Lecturer/Senior Lecturer/Professor in various institutions in India and U.K, from 2000 to 2006 and from 2010 to 2014. She has been with The Newcastle University in Singapore (NUIs), since 2014, where she is currently an Associate Professor in electrical power engineering, and also the Director of excellence in learning and teaching. Her research interests include renewable energy integration and applications in smart grid, power electronics for aerospace, electric vehicle applications, low carbon electrical energy systems, and power electronic solutions to sustainability.

Dr. Naayagi is a Steering Committee Member of NU Women, U.K., a member of the Diversity Working Group, Newcastle University, U.K., and Equality & Diversity Champion for NUIs, and an Academic Lead for Athena SWAN Bronze Award application at Newcastle University. She is a Senior Fellow of the Higher Education Academy, U.K. She has received several merit certificates for her academic proficiency, including the Best Outgoing Female Graduate Award during her bachelor's and the Outstanding Master's Student Award. She was a first recipient of the Dorothy Hodgkin Post-graduate Award from the School of Electrical and Electronic Engineering, University of Manchester, for her Ph.D., jointly sponsored by Rolls-Royce plc and the Engineering and Physical Sciences Research Council, U.K. She received the Woman Engineer Award from the Young Professionals Section Chennai, Institution of Engineering and Technology (IET), U.K., in 2012. She received the Newcastle University Teaching Award, in 2016. She is the Chair of NUIs women in science and engineering network and has been organizing many events to promote young professionals, especially young women in engineering and technology. She is the Chair of the IEEE Power and Energy Society, Singapore Chapter. She is an Associate Editor of the *IET Power Electronics* Journal and an Associate Editor of the *CSEE Journal of Power and Energy Systems*. She serves as a Reviewer for the IEEE, IET, and many other international journals and conferences.



**GAYADHAR PANDA** (Senior Member, IEEE) received the B.E. degree in electrical engineering from the Institute of Engineers, Kolkata, India, in 1996, the master's degree in power electronics from IEST, Shibpur, India, in 1998, and the Ph.D. degree in electrical engineering from Utkal University, Bhubaneswar, India, in 2007.

Since 2013, he has been with the Department of Electrical Engineering, National Institute of Technology at Meghalaya, Shillong, India, where he is currently a Professor. He served as the Head of the Department and the Chairman of various committees at the Institute level. He is currently looking after the Dean (FW), the Dean (AA), and a Chief Vigilance Officer (CVO) at NIT Meghalaya. He has published more than 80 technical articles in national and international conferences proceedings/journals. He has received the Institution Medal for obtaining the highest marks in graduation and the Power Medal for his one of the research article. He has more than 20 years of teaching experience. His current research interests include automatic generation control, stability improvements using flexible alternating current transmission system devices, power quality, power electronic converters, and distributed power generation.

...